Ice in the Environment: Proceedings of the 16th IAHR International Symposium on Ice
Dunedin, New Zealand, 2nd–6th December 2002
International Association of Hydraulic Engineering and Research

MODELLING OF REFROZEN CRACKS IN SEA ICE

Chris Petrich[1], **Pat J. Langhorne**[1] **and Tim G. Haskell**[2]

ABSTRACT
Refrozen cracks in sea ice provide the conditions that allow the investigation of refreezing saltwater ice under heat transfer in two dimensions. In this study we investigate the refreezing process of cracks with a numerical model based on the finite volume method with mushy layer treatment after Darcy. The model results are compared to our field data on refrozen cracks 10 to 40 cm wide. We find that numerical sea ice growth modelling is still handicapped by the absence of appropriate permeability parameterizations of the crystal structure. However, we are able to obtain qualitative agreement between model and reality.

INTRODUCTION
More than half of the global sea ice cover melts in summer only to freeze again in winter. During the growth season external forces, such as water currents, wind, waves, and thermal stress frequently break the ice apart. If the ice has the opportunity to refreeze under relatively calm conditions, cracks between the floes may freeze in a divergent regime and form the material for our studies. We have investigated the growth of cracks of 10 to 40 cm width in landfast, first–year ice in McMurdo Sound, Antarctica.

Sea ice growth is intrinsically difficult to model. Not only do different crystal structures form depending on the general sea conditions at the time, but the situation becomes more complicated due to the development of brine drainage channels (Cole and Shapiro, 1998), platelet ice (Smith et al., 2001), and the presence of snow. There are analytical approaches to model sea ice growth dating back over 100 years (Stefan, 1991), on top of which various refinements have been developed, and models have been tailored according to characteristics of specific regions (Crocker and Wadhams, 1989). All these models treat sea ice growth as essentially one–dimensional growth of an infinite ice sheet. Furthermore, two–dimensional and three–dimensional models have been used in the past to investigate one–dimensional sea ice growth. Those studies were mainly focused on the development of convection and brine drainage channels in the mushy layer, using sea ice or alloys as examples.

[1]Department of Physics, University of Otago, Dunedin, New Zealand
[2]Industrial Research Ltd., P.O. Box 31-310, Lower Hutt, New Zealand

The modelling targets in this study are freezing front development, brine inclusion alignment and salinity distribution. The incentive to model salinity stems from our observation of unexpected two–dimensional salinity profiles in excavated natural and artificial cracks (typically 10–40 cm wide). On some occasions we observed the highest salinities along the center of the crack, while on other occasions the center bore lower salinities than its surrounding. Brine inclusions and channels were found to align as arches (Petrich et al., in press), i.e. they tilt towards the colder side with increasing depth rather than towards the warmer side (probably similar to the observations of Niedrauer and Martin (1979)) as one might expect due to brine pocket migration. Further, measurements of the position of the freezing front at the center of narrow artificial cracks suggested freezing front advancement at a constant rate, unlike the square root dependence found in one-dimensional ice growth (Stefan, 1891).

The structure of naturally refrozen cracks is strikingly similar to the structure of artificial refrozen cracks that grew under our observation over about one week (Petrich et al., in press). We therefore neglect platelet ice formation and snow cover in our model, and assume that we can reach qualitative statements valid for both artificial cracks and natural cracks. In this paper we present results from our numerical model of sea ice growth in cracks.

NUMERICAL MODEL

Finite Volume Method

We attempt to model crack refreezing numerically with the finite volume method. To reduce computation we treat the refreezing problem two–dimensionally, i.e. we assume ice properties along the crack axis are homogeneous. The two–dimensional cross section is divided into a regularly spaced grid of finite volumes, each of them containing a local average of temperature T, salt concentration in the liquid fraction C (kg salt per m^3 liquid water), liquid volume fraction f, and pressure p. The local superficial velocity averages (i.e. volume fraction of the liquid times interdentritic velocity) in x–direction (u) and y–direction (v) are stored in a corresponding staggered grid (Patankar, 1980). The average physical properties of each cell are volume–fraction weighted averages of the properties of the liquid and solid. Motion of the liquid is determined by the incompressible Navier–Stokes equation, where the density is assumed constant with the exception of an advection source term (Boissinesq approximation). Motion in the mushy region in addition is hampered by a porous medium friction term after Darcy (D_x and D_y, respectively) that is based on the assumption that the flow rate is proportional to the pressure gradient. We neglect volume expansion during freezing and obtain governing equations for liquid transport that are similar to the ones used by Felicelli et al. (1991),

$$\rho_0\left[\frac{\partial u}{\partial t} + u\frac{\partial u}{\partial x} + v\frac{\partial u}{\partial y}\right] = \mu\left(\frac{\partial^2 u}{\partial x^2} + \frac{\partial^2 u}{\partial y^2}\right) - f\frac{\partial p}{\partial x} - f\, D_x\, u \quad \text{and} \tag{1}$$

$$\rho_0\left[\frac{\partial v}{\partial t} + u\frac{\partial v}{\partial x} + v\frac{\partial v}{\partial y}\right] = \mu\left(\frac{\partial^2 v}{\partial x^2} + \frac{\partial^2 v}{\partial y^2}\right) - f\frac{\partial p}{\partial y} - f\,\rho(T, S)\, g - f\, D_y\, v, \tag{2}$$

where ρ_0 is the density of water, and μ is the dynamic viscosity of water. D_x and D_y are Darcy coefficients ($D = \mu/\Pi$, where Π is the permeability) in units of $kg\,m^{-3}\,s^{-1}$ as

discussed below. Heat and mass transport follow the transport equations

$$\frac{\partial T}{\partial t} + u\frac{\partial T}{\partial x} + v\frac{\partial T}{\partial y} = \alpha\left(\frac{\partial^2 T}{\partial x^2} + \frac{\partial^2 T}{\partial y^2}\right) \quad \text{and} \tag{3}$$

$$\frac{\partial C}{\partial t} + u\frac{\partial C}{\partial x} + v\frac{\partial C}{\partial y} = \mathcal{D}\, f\left(\frac{\partial^2 C}{\partial x^2} + \frac{\partial^2 C}{\partial y^2}\right), \tag{4}$$

respectively, where α is the thermal diffusivity and $\mathcal{D}$ is the solute diffusion coefficient. It should be noted that experience of the authors of this paper and others (Patankar, 1980; Felicelli et al., 1991) shows that consistency in the formulation (Patankar, 1980) is far more important than the method to average the liquid volume fraction in a staggered grid. Local thermodynamic equilibrium is enforced at each time step by adjusting the liquid fraction according to

$$-L\,\frac{\partial f}{\partial t} = c\,\frac{\partial T}{\partial t}, \tag{5}$$

until the temperature reaches the local equilibrium freezing temperature $T_F(S)$. L is the latent heat of fusion, and c the volume averaged heat capacity. The salinity S (in psu) itself is a function of the liquid fraction f:

$$S = 1000 \times \frac{C_0 \frac{f(t_0)}{f(t_0+\partial t)}}{C_0 \frac{f(t_0)}{f(t_0+\partial t)} + \rho_0}, \tag{6}$$

if the density of the solid and of the liquid are equal, and the solute is completely rejected into the liquid. The pressure term is used to enforce mass conservation, and mass and momentum terms are coupled through either the iterative SIMPLER or SIMPLEC algorithm (Patankar, 1980; Versteeg and Malalasekera, 1995). In the following calculations the convective term is discretized with the first order upwind scheme, and the transient term is discretized with the second order Crank–Nicolson scheme.

Mushy layer

While the numerical modelling of laminar flows in a pure liquid is a standard task in computational fluid dynamics (CFD), no satisfactory description of the sea ice mushy layer seems presently available. In the past, several approaches have been used to cope with the dendritic mushy zones of sea ice and alloys. Among those that treat the liquid zone and the mushy zone with the same set of equations are formulations that use anisotropic permeability functions (Felicelli et al., 1991; McBride et al., 1999), isotropic permeability functions after Carman–Kozeny (Bennon and Incropera, 1987), and mixed formulations, where both the viscosity and the permeability depend on the liquid volume fraction (Medjani, 1996). Further, there is further evidence that in the case of sea ice, the permeability drops dramatically as the solid fraction exceeds 95 %. Given that the permeability depends on the liquid volume fraction, the crystal and grain structure (Worster, 1992), and the growth history (Golfier et al. 2002; Weeks and Ackley, 1982), we tried several approaches and decided to use an isotropic permeability term following Carman–Kozeny

$$D(f) = D_0 \frac{(1-f)}{f^3}. \tag{7}$$

To be accurate for small solid fractions one expects this equation to go linearly to zero (Schwarzer, 1995), which is not given for the classical Carman–Kozeny relationship for

porous media. Although the crystal structure is anisotropic within a refrozen crack, it changes from the long axis of the crystal aligned horizontally in the ice at the sides, to a vertically oriented columnar axis in the center (Petrich et al., in press), the crystal *c*–axes point along the crack justifying an isotropic approach in our two–dimensional model. For solidification from above, the existence of a critical depth, the point at which brine expulsion from the mushy region first sets in, is demonstrated by Wettlaufer et al. (1997) in laboratory experiments and field measurements (Wettlaufer et al., 2000) on sea ice. The critical depth is readily reproduced in our model if a solute diffusion coefficient of $D = 0$ is assumed. From the observations in Wettlaufer et al. (2000) we note that plume convection sets in at a critical depth of about 35 mm if the surface temperature is $-7°$ C. We use this fact to calibrate equation 7 and find $D_0 \approx 2 \times 10^7\,\mathrm{kg\,m^{-3}\,s^{-1}}$, a value that is consistent with permeabilities estimated and used by other authors (Wettlaufer et al., 2000; Feltham, 2002).

Numerical Results

As discussed in the previous section, there is no generally accepted permeability model of the mushy layer of sea ice at the present stage. Before discussing slots, we therefore present results of a one–dimensional calculation to illustrate that our approach to the mushy layer appears to be at least qualitatively sensible.

One-dimensional problem

We run the model on a one–dimensional problem of freezing seawater from above with a surface at constant temperature $-7°$ C, and the water ($S = 34$ psu) at the freezing point (T_F). We apply periodic boundary conditions at the sides, choose a domain 16 mm wide and 64 mm high, resolved in $0.5 \times 0.5\,\mathrm{mm}^2$. To avoid a substantial increase in salinity in the liquid domain we overwrite temperature and salinity data with the initial values in the bottom 4 mm after each time step. This procedure neither leads to numerical instabilities, nor to a discontinuity in the pressure correction field.

With this setup we find that brine plume release sets in after about 9700 s when the mushy layer has reached a thickness of 35 mm. During the following 2000 s we observe that brine channels of the width of one cell (0.5 mm) and free of solid remain at the locations of outflowing brine plumes and in fact grow in length back into the mushy zone by a further 5 mm. At the top of the upwards growing brine channels are funnel–like regions of increased average salinity that feed the brine channels. While the salinity of the brine channels is higher than that of seawater, their surroundings are depleted of salt. This kind of redistribution has been previously observed in laboratory experiments (Cottier et al., 1999). The channels exhibit continuous brine expulsion, although the flow rate oscillates somewhat.

Two-dimensional problem

Our two–dimensional problem is the refreezing of a slot sketched in Fig. 1a. We choose typical dimensions for a slot, i.e. 24 cm wide and 158 cm high. We assume a linear temperature gradient at the boundaries at the side, and a constant air–ice surface temperature T_0 of $-10°$ C. The entire domain is 176 cm high and resolved on a $1 \times 1\,\mathrm{cm}^2$ grid. The side walls of the bottom 18 cm are adiabatic, and we replace temperature and salinity data of the bottom 7 cm with the initial values after each time step.

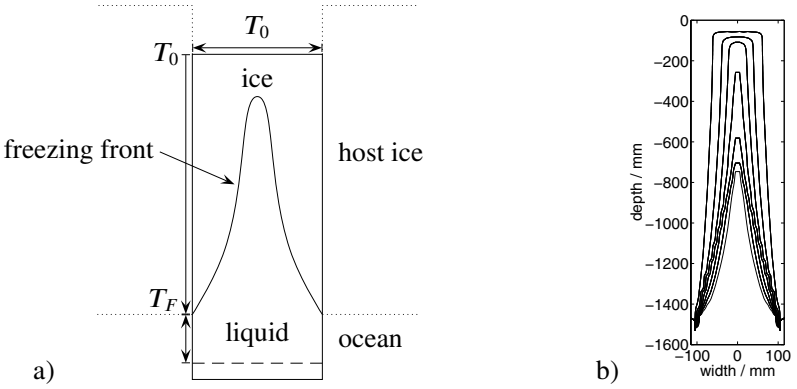

Figure 1: a) Schematic of the computational domain of the refeezing slot. Details are described in the text. For illustration, the shape of the host ice sheet and the position of the ocean are indicated by the dotted lines on both sides of the crack. b) Temporal development of the freezing front in model calculations for a surface temperature of $-10°$ C. The lines indicate the freezing front during the first 2 days in steps of 3×10^4 s. Note that the horizontal axis is stretched for clarity.

Our observations of artificial and natural cracks show brine drainage channels parallel to the freezing front (Petrich et al., in press). However, a two–dimensional growth model favors the development of brine channels perpendicular to the freezing front. Channels parallel to the interface require the freezing front to skip over a liquid section that is generally unstable due to convection in the liquid body. We have seen in calculations of the one–dimensional problem that growth parallel to the freezing front may be observable. However, we would not expect to be able to observe complex brine channel patterns in our calculations of a two–dimensional growth problem, particularly at a grid size of 1 cm.

During the initial stages of ice growth a weak (10^{-5} ms^{-1}) convection pattern develops with downwelling liquid at the sides and upwelling liquid in the center of the crack. This pattern is soon well established and persists throughout the freezing process, when liquid moves down at reduced velocities through the mushy layer at both sides. The lines of constant solid fraction soon develop an arch–like patterns as shown in Fig. 1b in keeping with experimental observations (Petrich et al., in press). The regions at the periphery of the slot desalinate with time due to slowly moving currents (less than 10^{-5} ms^{-1}) through the mushy layer. The movement towards the sides is in agreement with our field observation of a lack of discontinuity in the salinity profile between refrozen crack and bulk ice.

The center of the arched freezing front moves slowly downwards during the initial stages of refreezing, when heat transfer at the center is predominately towards ice–air interface. Once ice growth from the sides has reached the center of the crack, the top of the arch moves down considerably faster until it approaches the bottom of the domain (see Fig. 2a at 1.2×10^5 s). Fig. 3a and Fig. 3b show calculated salinity profiles for surface temperatures of $-25°$ C and $-10°$ C, respectively. For comparison, Fig. 3c shows the salinity profile of *slot* 1. In that experiment an air inclusion 60 mm wide and 60 mm below the

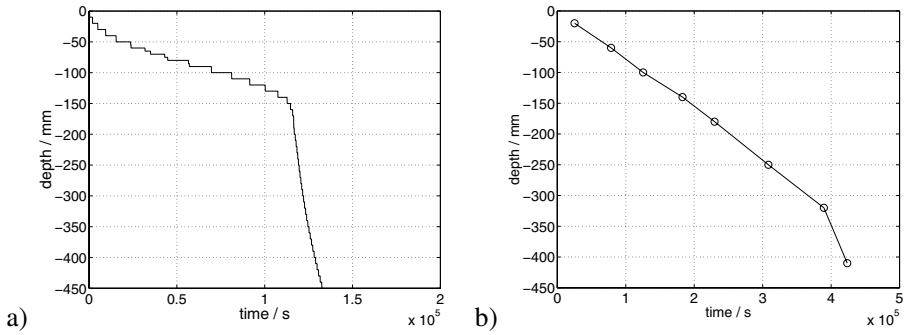

Figure 2: Position of the topmost point of the freezing front during refreezing. a) Data from the CFD model assuming a constant surface temperature of −10° C. b) Data from refreezing experiment *slot* 1. Note the different time axes for the plots.

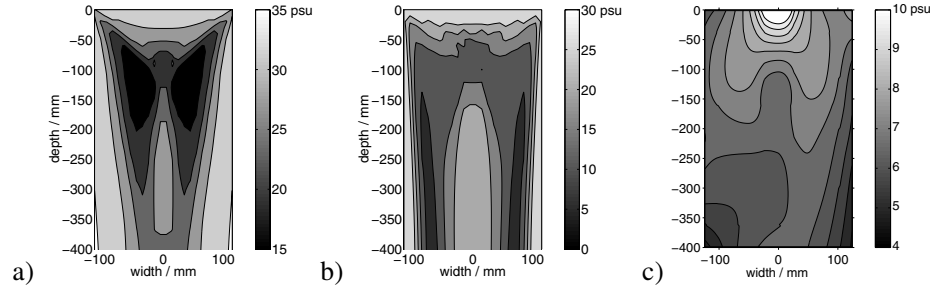

Figure 3: Top section of the vertical salinity profile through refrozen slots. a) Data from the CFD model after 1 day assuming a constant surface temperature of −25° C. b) Data from the CFD model after 2.5 days assuming a constant surface temperature of −10° C. c) Interpolated data from refreezing experiment *slot* 1 after 4 days. Note that the salinity range in the plots differs.

surface may have influenced the salinity profile. The generally higher salinities in the model may be partly due to the fact that pressure–driven brine expulsion as a result of volume expansion has been neglected.

FIELD OBSERVATIONS

We have investigated natural refrozen cracks and artificial cracks, i.e. slots 2 to 3 m long cut into the ice, on landfast sea ice in McMurdo Sound, Antarctica during spring, in October and November. In natural refrozen cracks, the top 30 cm were cut out with a chain saw, then sectioned into pieces 8 cm high, 5 cm wide, and 12.5 cm along the crack axis, melted, and the salinity was measured (see Petrich et al., in press, for more details). In slot refreezing experiments we have measured the freezing progress with a thermistor probe, and obtained a salinity profile at the end of the experiment as in the case of natural refrozen cracks.

The position of the top of the advancing arch in experiment *slot* 1 is shown in Fig. 2b.

One notices that the freezing front appears to accelerate at about 350 mm, after a period of linear advance. Additional data, not reproduced here, show that this is the point at which the arch becomes very steep, which agrees with the observation from the numerical model. By comparison, the model (Fig. 2a) seems to exaggerate the influence of ice growing from the sides, which leads to a change in slope at smaller depths than observed in nature. This may be a consequence of the assumption of a linear temperature gradient at the sides that remains constant over time.

The top 350 mm of the measured salinity profile in Fig. 3c shows a center that is surrounded by ice of higher salinity. In our field observations on natural refrozen cracks about 20 cm wide we also observe a region of depleted salinity at the center in the topmost 30 cm. On the other hand, the region below this, and narrower cracks (e.g. 8 cm wide) exhibit a higher salinity at the center. We attribute this difference to differences in the convection pattern or growth velocity. The appropriate comparison between the calculation of Fig. 3b and the experimental data of Fig. 3c is made at the depth of the change in slope in Fig. 2a and Fig. 2b. That is at approximately 150 mm and 350 mm in Fig. 3b and Fig. 3c, respectively. At these depths and below the salinity can be seen to be largest at the center of the crack, dropping in value towards the edges, showing qualitative agreement between model and experiment.

SUMMARY AND CONCLUSION

We have introduced a numerical model to simulate the freezing process of sea ice in cracks. Qualitatively, a variety of observations made in field experiments could be reproduced. On a small scale, brine drainage features and salt redistribution were observed. With respect to cracks the freezing front development was confirmed. A current has been observed moving seawater up the center of the crack, and down along the freezing front and inside the mushy layer. This current seems to affect the salinity distribution in the refrozen crack. Definite quantitative statements regarding salinity and current velocities are precluded at this stage owing to the absence of a quantitative permeability model of sea ice.

ACKNOWLEDGEMENT

The authors wish to say thanks for their great support to Dave Hardisty, Myles Thayer, Barbara Buchanan, Peter Stroud, Dale Watts, and Dr. Colin Wells in preparation of the experiments, and in the field to Dr. Dave Cole, Dr. Jean–Louis Tison, Dave Cochrane, Simon Gibson, Eberhardt Deuss, Jonathan Leich, to Scott Base staff, and to Antarctica New Zealand.

REFERENCES

Bennon, W.D. and Incropera, F.P. A continuum model for momentum, heat and species transport in binary solid–liquid phase change systems–II. Application to solidification in a rectangular cavity. *International Communications on Heat and Mass Transfer 30*(10): 2171–2187 (1987).

Cole, D.M. and Shapiro, L.H. Observation of brine drainage networks and microstructure of first–year sea ice. *Journal of Geophysical Research 103*(C10): 21739–21750 (1998).

Cottier, F. Eicken, H. and Wadhams, P. Linkages between salinity and brine channel dis-

tribution. *Journal of Geophysical Research 104*(C7): 15545–15557 (1999).

Crocker, G.B. and Wadhams, P. Modelling Antarctic fast–ice growth. *Journal of Glaciology 35*(119): 3–8 (1989).

Felicelli, S.D., Heinrich, J.C. and Poirier, D.R. Simulation of freckles during vertical solidification of binary alloys. *Metallurgical. Transactions B 22B*: 847–859 (1991).

Feltham, D.L., Worster, M.G. and Wettlaufer, J.S. The influence of ocean flow on newly forming sea ice. *Journal of Geophysical Research 107*(C2), 3009, doi: 10.1029/2000JC000559 (2002).

Golfier, F., Zarcone, C., Bazin, B., Lenormand, R., Lasseux, D. and Quintard, M. On the ability of a Darcy–scale model to capture wormhole formation during the dissolution of a porous medium. *Journal of Fluid Mechanics 457*: 213–254 (2002).

McBride, E., Heinrich, J.C. and Poirier, D.R. Numerical simulation of incompressible flow driven by density variations during phase change. *International Journal for Numerical Methods in Fluids 31*: 787–800 (1999).

Medjani, K. Numerical simulation of the formation of brine pockets during the freezing of the NaCl-H_2O compound from above. *International Communications on Heat and Mass Transfer 23*(7): 917–928 (1996).

Smith, I.J., Langhorne, P.J. Haskell, T.G., Trodahl, H.J., Frew, R. and Vennell, M.R. Platelet ice and the land–fast sea ice of McMurdo Sound, Antarctica. *Annals of Glaciology 33*: 21–27 (2001).

Patankar, S.V. *Numerical Heat Transfer and Fluid Flow.* Hemisphere Publishing Co. NY (1980).

Schwarzer, S. Sedimentation and flow through porous media – simulating dynamically coupled discrete and continuum phases. *Physical Review E 52B*(6): 6461–6475 (1995).

Stefan, J. Über die Theorie der Eisbildung, insbesondere über die Eisbildung im Polarmeere. *Annalen der Physik, 3rd Series 42*: 269–286 (1891).

Versteeg, H.K. and Malalasekera, W. *An Introduction to Computational Fluid Dynamics.* Pearson Education Ltd., London (1995).

Wettlaufer, J.S., Worster, M.G. and Huppert, H.E. Natural convection during solidification of an alloy from above with application to the evolution of sea ice. *Journal of Fluid Mechanics 344*: 291–316 (1997).

Wettlaufer, J.S., Worster, M.G. and Huppert, H.E. Solidification of leads: Theory, experiment, and field observations. *Journal of Geophysical Research 105*(C1): 1123–1134 (2000).

Weeks, W.F. and Ackley, S.F. *The Growth, Structure, and Properties of Sea Ice*, CRREL Monograph 82–1, Hanover, N.H. (1982).

Worster, M.G. Instabilities of the liquid and mushy regions during solidfication of alloys. *Journal of Fluid Mechanics 237*: 649–669 (1992).